Measurement 144 (2019) 72–82

Contents lists available at ScienceDirect

Measurement

journal homepage: www.elsevier.com/locate/measurement

Hybrid adaptive algorithm based on wavelet transform and independent component analysis for denoising of MRI images

Hari Mohan Rai *, Kalyan Chatterjee

Department of Electrical Engineering, Indian Institute of Technology (ISM), Dhanbad, Jharkhand, India

ARTICLE INFO

Article history:
Received 24 January 2016
Received in revised form 30 March 2019
Accepted 9 May 2019
Available online 15 May 2019

Keywords:
DWT
ICA
MRI
MSSIM
PSNR
UDWT

ABSTRACT

This paper proposes a novel approach for elimination of noises from MRI images using hybrid adaptive algorithm based on DWT and ICA. MRI images are usually corrupted by various types of noise which reduces the accuracy of any automatic analysis system. So, the denoising methods always used to increase the PSNR and MSSIM of images to improve the originality. The MRI data used was corrupted by gaussian noise, speckle noise, salt & pepper noise respectively. The noise density to MRI Images was added noise variance from 10% to 90% to compare the performance of the denoising methods. The proposed hybrid adaptive algorithm has been used by combining WT and ICA techniques to remove the noise from MRI images. The statistical parameters such as PSNR and MSSIM are used to compare the performance of the proposed technique. The proposed technique is compared with conventional techniques, such as DWT, UDWT, and ICA.

© 2019 Elsevier Ltd. All rights reserved.

1. Introduction

Images are considered as a powerful source of information and widely used in numerous fields. For example, in the medical industry, machine vision, and space exploration etc. The field of image processing is thus considered to be very complex and of diverse nature. Due to this, image processing is one of the most challenging areas in mathematics, engineering, medical science, and entertainment industry. Development of computer technology enables us to process images produced by devices such as camera, scanner, ultrasounds, and machine vision system to improve their quality, enhance their features, and combine different pieces of information. Machine vision is one of the most fascinating practices of image processing area and it has multiple divisions. Medical images, radar-based imaging, and SAR images are among those areas. In this perspective, the application of medical image analysis has been of great interest to the researchers. Artificial intelligence and machine intelligence are two main types of intelligence, where machine intelligence is mainly used in the electronic systems.

Noise alters the original information of the image and it is stated as the random variation of intensity of a pixel of images. As a result, pixels which appear in the image are not the actual pixels. There are various types of noises categorized into Gaussian noise, uniform noise, salt and pepper noise also called impulse noise, speckle noise, gamma noise, photon noise and exponential noise etc [1].

Gaussian noise arises in detectors or amplifiers hence it is also known as electronic noise. It is produced by natural cause like warm objects radiations and its discrete nature and atoms thermal vibration. Salt and pepper noise or impulse is also known data drop noise since it uses to drop the values of original data [2].

The noise that generated during acquisition of images because of the effect of environmental circumstances on the sensor of an imaging device is known as speckle noise. It mostly appears incoherent imaging such as medical images, SAR images and active radar images which is multiplicative in nature [1]. The clinical MRI data is normally corrupted by noises from the measurement processes. These noises reduce the accuracy and reliability of any automatic analysis system for abnormality detection. So, the noise reduction methods are employed to reduce the noise contents from images and thereby increase image quality. Noise removal methods are used for automatic diagnosis of MRI images such as for brain tumor detection, cancer detection etc. The noisy data may lead to the unsatisfactory result and cause a diagnostic error which led to the medical error. Diagnostic error is a very serious patient safety issue.

Abbreviations: DWT, discrete wavelet transform; ICA, independent component analysis; UDWT, undecimated discrete wavelet transform; MRI, magnetic resonance imaging; MSSIM, mean structure similarity index metrics; PSNR, peak signal to noise ratio; MSE, mean square error.

* Corresponding author.
E-mail address: harimohanrai@gmail.com (H.M. Rai).

https://doi.org/10.1016/j.measurement.2019.05.028
0263-2241/© 2019 Elsevier Ltd. All rights reserved.

In past few decades, there are several works have been presented on noise removal of MR images, even though the structural similarity and SNR of MR images are still a big concern. Therefore, elimination of noises from medical images is still a challenging task. Noise reduction in SAR and MRI imaging uses an important concept known as CFAR (constant false alarm rate). CFAR detection refers to constant false alarm rate, which is utilized to detect a target in an atmosphere of variable background noise in SAR and radar systems. Depending on the application, each of denoising, detection, segmentation, and classification, or a combination of them, is used in SAR and also in MRI imaging [3–7].

In recent years, several researchers have conducted various studies on noise removal of medical images, especially on MR images. Salimi-khorshidi et al. presented an automatic noise removal method of functional MRI using ICA and hierarchical fusion of classifiers [8]. A review on various denoising methods on MR images has been done by Mohan et al. Introduction to MRI and the noise characteristics in MRI and popular denoising methods were classified in the paper [9]. Denoising techniques, advantages and limits of MRI images were also deliberated in the study. Ai et al. have done the study on eleven type of typical image filters for MR images denoising. From the comparison of various noise removing filters for magnetic resonance images, they found that the Unbiased Non-Local Means is the superior for the phantom image with objective judgment, while with subjective judgment BM3D SAPCA is better to other filters for the clinical image [10]. Another method for noise suppression of MR image is a combination of Non-Local Means (NLM) filter with suitable fuzzy cluster criterion proposed by Bin Liu et al. This method revealed that it suppresses noise more effectively as compared to the simple NLM and wavelet method [11]. Random sampling non-local mean (SNLM) algorithm to remove the noise in 3D MRI datasets have been presented J Hu et al. NLM algorithms implemented have the drawback of high computational complexity [12]. Iterative nonlocal means filter (INLM) was proposed by Wang et al. to remove the salt and pepper noise from the images [13].

Kumar and Diwakar presented a new method to eliminate noise from computed tomography (CT) and tetrolet domain used to preserve the edge [14]. They also compared their proposed method with some standard denoising techniques in terms PSNR, MSE, and Image Quality Index (IQI). Lu et al. explained noise reduction of impulse noise using pixel variation and gain factor amended by a noise-free pixel number. The gray level value of non-extreme pixels are arranged in an increasing order and according to the variation of gray level these pixels are grouped. To determine the gain factor value, the median and distribution ration value are determined of each group. The weighted value are obtained by multiplying with each groups median value, these are replaced with middle pixels of extreme gray level value and enabling reconstruction of noise degraded pixels [15]. The noise reduction on imaginary and real part of the images (complex domain) was proposed by Baselice et al. This method used maximum a posteriori estimator for analyzing the complex images and for modeling this estimator [16]. Gai et al. employed a new algorithm for elimination of speckle noise from ultrasound images using bayesian framework and MWT (monogenic wavelet transform). In this study, laplace mixture distribution was computed from speckle noise signal and MWT coefficients of denoised signal and also determined rayleigh distribution. Then, the mean square error minimum value was computed using bayesian estimator for eliminating speckle noise. Lastly, parameters of the speckle noise reduction algorithm was estimated by means of the expectation maximization algorithm [17].

MRI signal noise reduction using robust PCA was explained by Zhu, Zhang, and Wang [18]. This method, significantly increases the temporal SNR and sensitivity of ASL (Arterial spin labeling) perfusion MRI images. A survey on various noise elimination techniques of CT images was discussed by Diwakr and Kumar. This study also presented the advantages and disadvantages of CT image noise reduction method [19]. Sudeep et al. proposed the NLML estimator (nonlocal maximum likelihood) for denoising of non-stationary noise of MR images. In this method, before maximum likelihood estimation, a noise map is determined using robust noise estimator. This study also introduces LFD (local frequency descriptors) based on similarity measure to compute the NL samples of ML approximation [20].

All the above methods have significant contribution in their specific application but neither of them is an adaptive method of denoising. Also, denoising of medical images should have high PSNR as well as high MSSIM to keep the image information unchanged. Many denoising methods studied above is either having high PSNR or high MSSIM, not both high.

In this paper, the denoising of MR images has been made by a novel hybrid technique using DWT-ICA. The proposed methodology is adaptive in nature which automatically adjusts the thresholding value depending upon the noise level. The parallel processing of the images can be done using the proposed method which reduces the computation time considerably. The method proposed can be applied for denoising of any kind of medical images having different types of the noise level. This method also gives high MSSIM and high PSNR values at the different level of noise density. This study utilizes the original dataset from charak diagnostic & Research center, Jabalpur, M.P., India [21].

The organization of the manuscript is as follows: MRI and its database is discussed in Section 2. Section 3 describes about the independent component analysis (ICA). Preprocessing of MR images using centering is explained in Section 4. In Sections 5 and 6, the methodology and of the proposed techniques are described.

2. Magnetic Resonance Imaging (MRI)

Magnetic Resonance Imaging (MRI) gained its significance from the early 1980s. Since then this medical imaging technique has proved itself to be valuable for the examination of the soft tissues of the body. An MRI scanner uses the phenomena of nuclear magnetic resonance i.e. it uses magnetic and radio waves, thus there is no risk of exposure to X-rays or any other damaging forms of radiations and a detailed picture of the inside of the human body can be obtained. The MRI scanner creates a radio magnetic field which is applied to the body part being exposed. The body's atoms are affected by this field and this field raises their energy level. When the field is removed these atoms relax and they send out radio waves of their own. The MRI scanner picks up these signals and a computer turns them into a picture. The Human body consists mainly of water, and water contains hydrogen atoms so the nucleus of the hydrogen atom is often used to create an MRI scan in the manner described above. The tissues having least number of hydrogen atoms (such as bones) turns out dark while the tissues that have many hydrogen atoms (such as fatty tissue) looks much brighter. An MRI scan is able to provide clear pictures of parts of the body that are surrounded by bone tissue, so the technique is useful when examining the brain and spinal cord [22–24].

There are three basic types of MRI scans, the T1 weighted images demonstrate excellent anatomic detail but do not show good contrast between normal and abnormal tissues. On the other hand, T2 weighted images provide excellent contrast between normal and abnormal tissues, although the anatomical details are less than that of T1 weighted images. The PD weighed scans have no contrast from either of the T1 or T2 weighted scans it only has the signal change coming from the difference in a number of available spins [25]. The T1 and T2 weighted MRI scans of the brain are

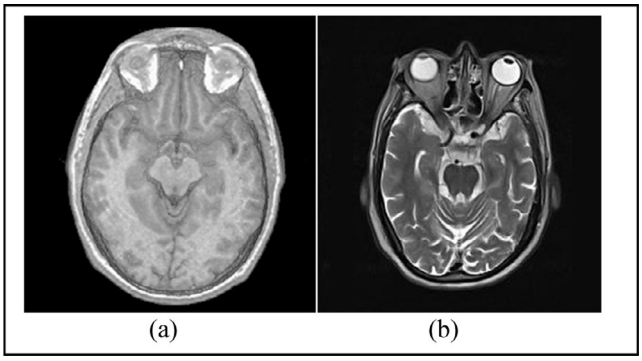

Fig. 1. (a) T1 weighted (b) T2 weighted MRI scans of the brain.

shown in Fig. 1. The MRI's have become an important radiological technique that is been used to visualize internal structure of the body. But it is still a challenging problem to extract the relevant clinical information to improve or even automate the diagnosis process. Denoising is a crucial step required for the MRI images depending upon the specific diagnosis tasks, high spatial resolution, and high contrast may be required. Whereas various image processing applications require a high SNR value because most of the algorithms are very sensitive to noise.

2.1. MRI database

The collection of data is first and most important part for any kind of image processing system. The real time MRI images of patients were collected for preparation of database to be used in this paper. The images were provided by Charak diagnostic & research center, Jabalpur, M.P., India. The database consists of images acquired from different body parts like Brain, Shoulder, Spine, Cardiac and Knee MRI's. One of the least accessible and most complex organ, the human brain is a primary beneficiary of magnetic resonance imaging technique, therefore the MRI images of brain were used in this manuscript. The selected test images consist of T1 & T2 weighted brain MR images in axial plane with 256×256 resolution having 27 slices from 9 patients. The MRI brain images used in this paper are of high contrast and noise free images to test the algorithm [21].

3. Independent component analysis (ICA)

ICA is also considered as one of the methods for solving the blind source separation (BSS) problem, it is used for separating data into informational components, where such data can take the form of images, sounds, telecommunication channels etc. Blind source separation means that such methods can separate data into source signals even if very little is known about the nature of those source signals. ICA is based on assumption that if different signals are from different physical processes then those signals are statistically independent considering this fact a new assumption is made by reversing the original as if statistically independent signals can be extracted from signal mixtures then these extracted signals must be from different physical processes. ICA separates mixed signals into statistically independent signals, each of the signals extracted by ICA has been generated by a different physical process, and will, therefore, be the desired signal. The ICA method is been applied to problems in various fields as speech processing, brain imaging (e.g., MRI and optical imaging), electrical brain signals (e.g., EEG signals), etc. From the above analysis, it was observed that independent component analysis is based on the assumption that different physical processes generate outputs that are independent of each other [26].

In real-world conditions, the numbers of signal mixtures are often larger than the number of source signals. For example, with electroencephalography (EEG) the number of different signal mixtures of a single set of source signals is equal to the number of electrodes on the head (usually greater than 10), and the number of sources is typically less than 10. For such conditions where the number of source signals is known and less than the number of signal mixtures then the number of signals extracted by ICA can be reduced by preprocessing the signal mixtures using principal component analysis [26,27].

For accurate diagnosis of magnetic resonance imaging, the MR image should clearly distinguish between different brain tissues, such as white matter tracts and gray matter. The standard MRI images are not able to show different tissues in detail. But, it is possible to use different MRI settings such that each setting captures a different mixture of the source signals associated with different tissues of interest. A simple mathematical representation of ICA model is as follows:

$$X = AS \tag{1}$$

where,

X = random vector with $n \times m$ elements
A = unknown mixing matrix.
S = Independent components.

The inverse of the matrix A is computed and it's denoted by W. The independent components are estimated by determining a separating matrix W. The separating matrix W is also known as demixing matrix, determined using an algorithm that optimizes iteratively statistical independence of the components of the mixture. The algorithm performing ICA that we have used is Fast ICA algorithm [26,28].

4. Preprocessing of data

Before the application of ICA algorithm, it is essential to preprocess the data. The preprocessing steps are described as follows:

4.1. Centering

The most basic and necessary preprocessing operation is to center the data, i.e. subtract its mean vector $m = E\{x\}$ so as to make the data a zero-mean variable. This entails that S is zero-mean as well. This preprocessing is prepared exclusively to simplify the ICA algorithms. The basic block diagram of centering operation is shown in Fig. 2.

4.2. Whitening

Whitening the data means data is transformed in such a way that the components are uncorrelated and have unit variance, and it is the second step of the preprocessing step. One way to

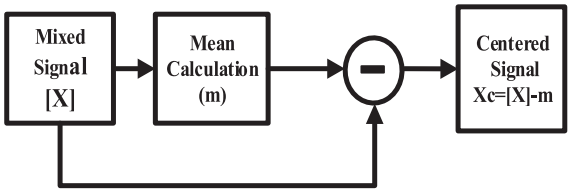

Fig. 2. Block diagram of centering operation.

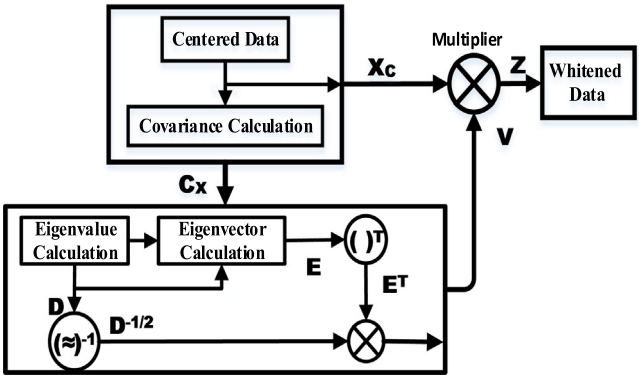

Fig. 3. Block diagram of whitening operation.

obtain the transformation matrix for whitening the data is by singular value decomposition. Whitening operation block diagram has been shown in Fig. 3.

C_X is a covariance matrix, for a zero-mean random vector X with n elements, is given by:

$$C_X = E\left\{XX^T\right\} = EDE^T \tag{2}$$

where E is a matrix containing the orthogonal matrix of eigenvectors (e_1,e_2,...,e_n) of a covariance matrix C_X and D is a diagonal matrix containing the corresponding eigenvalues of C_X.

The transformation matrix (whitening matrix) V that projects observed data X to whitened data Z is found as:

$$V = D^{\frac{-1}{2}} \times E^T \tag{3}$$

The whitened data is then obtained using this transformation matrix as:

$$Z = V \times X_C \tag{4}$$

X_C is the centered data after subtracting zero mean obtained from Fig. 2. Demixing matrix using Fast ICA algorithm is obtained after the preprocessing of data [26]. The demixing matrix of the independent components are then obtained as:

$$\widehat{S} = EZ = E \times VX = ED^{-1/2}E^TX = W \times Z \tag{5}$$

These independent components are then used to get the original ICA transformed components and produce acceptable denoising results.

5. Methodology

The proposed methodology presented for denoising of noisy MRI images in the following steps. First, an MRI image is chosen from the database [21] and its noisy version is obtained by corrupting the image from three types of noise available, white gaussian noise, salt and pepper noise and speckle noise respectively. The images are corrupted using five noise variance levels ranging 0.1, 0.3, 0.5, 0.7, and 0.9 that means corrupted with five noise density of 10%, 30%, 50%, 70% and 90% [15,17,29,30]. Various types and various levels of noise were added to figure out that proposed method can be used for denoising of MRI images which are corrupted by any types of noise. This method also proves that on the higher levels of noises it performs well as compared to other transform domain methods. The methodology of proposed technique is described in the following subsection.

5.1. Proposed (DWT-ICA) algorithm

Before the application of ICA to the MR images, we need to first preprocess the data. There are two steps in preprocessing the data i.e. centering and whitening. Centering the data is similar to the normalization of dataset which is the preceding step of whitening and another preprocessing step in ICA. Before applying the ICA and after centering the data, it is required to observe vector X, it should be linearly varying so that the obtained vector $\widehat{X}$ should be white, i.e. this component should be uncorrelated and its variance should be equal to unity.

The demixing matrix W using the fast ICA algorithm were found after completion of preprocessing steps [24]. This algorithm works on the principle of artificial neuron, having a weight vector "w" that the neuron is able to update by a learning rule. The value of w is selected in such a way that it maximizes nongaussianity of the projection w^TX, where $X \in R^{N\times M}$. Non-Gaussianity measure, depends the function u which is nonlinear and nonquadratic, g is the 1st derivative and g_0. According to the [31] the function u is defined as:

$$u = logcosh(u), g = tanh(u),\ g_0 = 1 - tan^2h(u) \tag{6}$$

The Flowchart of the proposed algorithm (DWT-ICA) is shown in Fig. 4. and explained in details as:

Step 1: Take the noisy MR images.

Step 2: Preprocess the data using centering and whitening operation.

Step 3: Choose an initial (e.g. random) weight vector w, here w is a column-vector $w \in R^N$.

Step 4: Let $w^+(k) = E\{Xg(w^TX)\} - E\{g_0(w^TX)w\}$

$w^+(k)$ is a temporary or momentary variable used to calculate w. Updated or new weight vector at each step is expressed as $w^+(0)$, $w^+(1)$ .... $w^+(n)$. $g_0(.)$ and $g(.)$ are defined in Eq. (6) and $E(.)$ is the mean averaging of column-vectors of the whitened data X.

Step 5: Let $w(k) = \frac{w^+}{w^+}$ Where $w(k)$ is the column weight matrix and k denotes the number of iteration.

Step 6: Go back to step 4 if data does not converge. Convergence means, the previous and updated values of weight vector point w should be in the similar direction, i.e. the dot product of both vale should be approximately equal to 1.

Step 7: The next step of the algorithm is to find the demixing matrix 'W' which maximizes the given measure of non-gaussianity of the sources 'S'. Demixing matrix each column can be identified as the center patch of one independent component. The independent components are obtained by using equation as:

$$\widehat{S}_{Noisy} = W \times Z \tag{7}$$

If the demixing matrix estimate is accurate, then good approximation of the independent components can be obtained.

Step 8: Since the noisy data were used for estimation of the independent components so the estimates obtained are the noisy estimates and it is required to obtain the estimates which contain minimum noise. So, these independent components are then decomposed using discrete wavelet transform using the daubechies 3 as a wavelet function of level 5.

Step 9: Thresholding is now applied to the detail components; a shrinking nonlinearity is applied based on threshold value calculated using Visushrink thresholding function. Visushrink thresholding is the automatic soft thresholding method used in WT. It is adaptive and powerful thresholding method which results very smooth with a pleasant visual appearance. VisuShrink uses the Universal threshold, "V", which is proportional to the standard deviation of the noise, is defined as

$$V = \sigma\sqrt{2\log N} \tag{8}$$

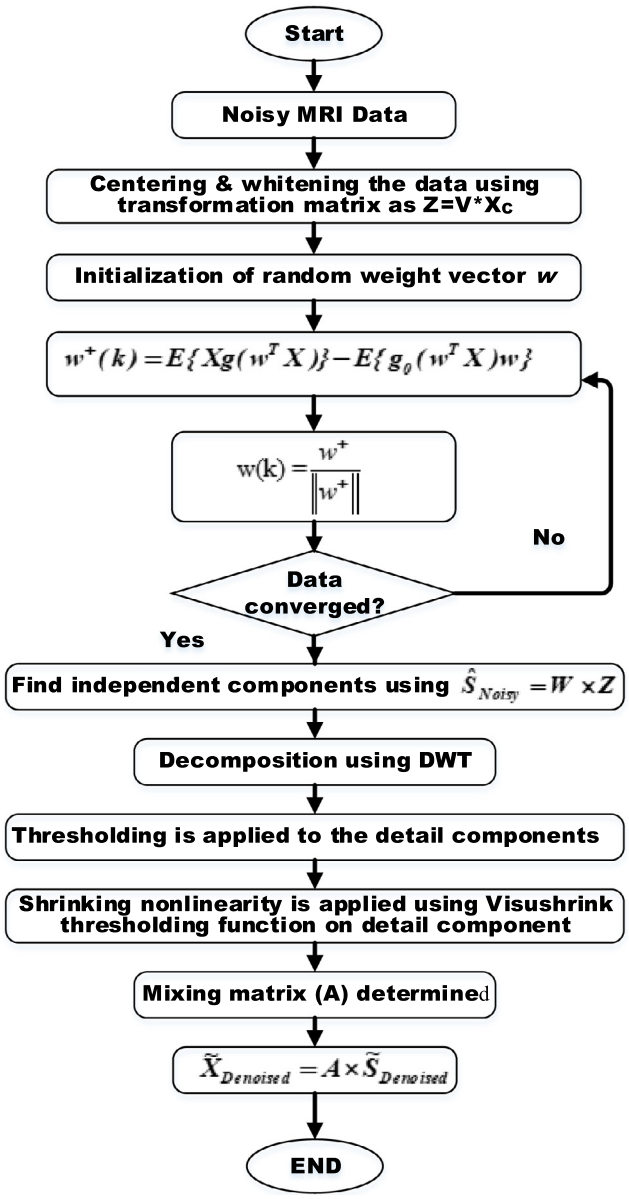

Fig.4. Flowchart of proposed algorithm (DWT-ICA).

where σ represents the noise variance level of an image and "*N*" representing the total number of pixels [32,33].

Step 10: The demixing matrix *W* obtained from Eq. (7) is utilized to determine the mixing matrix *A*, which is the inverse of the demixing matrix *W*. Lastly, the denoised image is then obtained by using the mixing matrix and the denoised independent components as:

$$\tilde{X}_{Denoised}=A\times\tilde{S}_{Denoised} \tag{9}$$

The proposed algorithm uses discrete wavelet transform is used along with ICA and combined them based on the approximations on DWT decomposition. The reason behind combining DWT with ICA is that the DWT downsamples the detail and approximation coefficients at each decomposition level where as downsampling operations does not incorporated in UDWT. Due to this the decomposition step using daubechies 3 wavelet will not be possible if we use UDWT and will not be efficient and effective.

However the denoising with the UDWT gives better denoising result as compare to DWT because UDWT has the shift-invariant or translation-invariant property. Also the noise reduction result using UDWT has improved balance between precision (accuracy) and smoothness than the DWT [34].

5.2. Analysis of denoising capability

To analyze the quality of the denoised image obtained by the proposed algorithm explained in the previous section, two types of standard image quality measure have been used. Peak signal to noise ratio (PSNR) and mean structural similarity index metric (MSSIM) have been utilized in this paper.

5.2.1. Peak signal-to-noise ratio (PSNR)

The PSNR is abbreviated as peak signal-to-noise ratio and it is defined as the ratio between the maximum likely power of a signal and the power of corrupting noise that affects the fidelity of its representation. The PSNR is used as an evaluation of the quality of reconstruction of an image. A high value of PSNR normally indicates that the reconstructed images are of high quality. PSNR defined via the mean squared error (MSE) which uses two $m \times n$ monochrome images I (original image) and K (noisy/denoised image) is defined as: The PSNR is defined as [15]:

$$MSE=\frac{1}{mn}\sum_{i=0}^{m-1}\sum_{j=0}^{n-1}[I(i,j)-K(i,j)]^2 \tag{10}$$

$$PSNR=20\log_{10}\left(\frac{MAX_I^2}{MSE}\right) \tag{11}$$

Here, MAX_I is the maximum possible pixel value of the image. If the pixels are symbolized using 8 bits per sample, this value is 255.

5.2.2. Mean structural similarity index metric (MSSIM)

The technique for measuring the similarity between two images is known as structural similarity (SSIM) index. Generally, traditional methods of the quality measure of images like PSNR and MSE were improved by SSIM. MSE and PSNR techniques are used for estimating perceived errors, on the other hand, SSIM is the measure of image quality degradation as perceived change in structural information. In other words, the SSIM is the measure of originality testing of reconstructed noisy images. The SSIM metric is calculated on various windows of an image, The measure between two windows x and y of common size $N \times N$ is it is given as [35]:

$$\mathrm{SSIM}(x,y)=\frac{(2\mu_x\mu_y+c_1)(2\sigma_{xy}+c_2)}{\left(\mu_x^2+\mu_y^2+c_1\right)\left(\sigma_x^2+\sigma_y^2+c_2\right)} \tag{12}$$

where μ_x the average of x; μ_y the average of y; σ_x^2 the variance of x; $\sigma_y^2$the variance of y; σ_{xy} the covariance of x and y.

C1 and C2 are two variables to stabilize the division with weak denominator

$$MSSIM(X,Y)=\frac{1}{M}\sum_{j=1}^{M}SSIM(x_j,y_j) \tag{13}$$

where X and Y are original and noisy/denoised images, respectively; x_j and y_j are the image contents at the jth local window; and M is number of local windows in the image.

Mean structural similarity index metric is the mean value of SSIM. The resultant MSSIM value is a decimal value between 0 and 1, where "0" indicates no matching between original images with denoised images and value "1" indicates the 100% matching with original images means the two images are identical [15].

6. Experimental results

In this section the result obtained using proposed technique is explained, verified and compared for denoising of actual data obtained from seimens 1.5 T clinical scanner. The experimental results are accomplished on a T1-weighted seimens 1.5 T MRI images using MATLAB software package R2011b. Two important statistical parameters metrics (PSNR and MSSIM) are used to demonstrate the comparison of the proposed method with other transform domain methods. The simulation results calculated by denoising the MRI images using the DWT-ICA method are demonstrated and compared with other techniques such as DWT, UDWT, and ICA.

To begin with experiment first an MR image was chosen from the database and Gaussian noise, salt & pepper noise, and speckle noise are added to the image. The noise variance level added to the MR image ranges from 0.1 to 0.9.

The MR image corrupted by Gaussian noise, speckle noise, salt & pepper noise with noise variance from 0.1 to 0.9 was denoised using the proposed method. Then the same noise corrupted image was filtered using discrete wavelet transform, undecimated discrete wavelet transform and independent component analysis to provide a baseline comparison. To evaluate the performance of the proposed method, PSNR and MSSIM value is determined as a quality metric. Fig. 5 shows the denoising performance of the various methods by plotting the line graph between output PSNR values calculated from denoised MRI images corrupted by Gaussian noise and different noise variance. It can be visualized that the proposed method offers better result as compared with UDWT, DWT, and ICA by means of the higher PSNR values for different noise density. It is also noticeable that UDWT gives better performance in terms of PSNR as compared to DWT and ICA.

Along with PSNR, the MSSIM values for different noise variances (0.1, 0.3, 0.5, 0.7 and 0.9) were also obtained to demonstrate the similarity between the original image and denoised image, shown in Fig. 6. It picturizes that the MSSIM value is largest for proposed method among all other techniques at lower noise variance level i.e. the proposed algorithm is capable of restoring the images without losing much information. But at higher noise level especially at

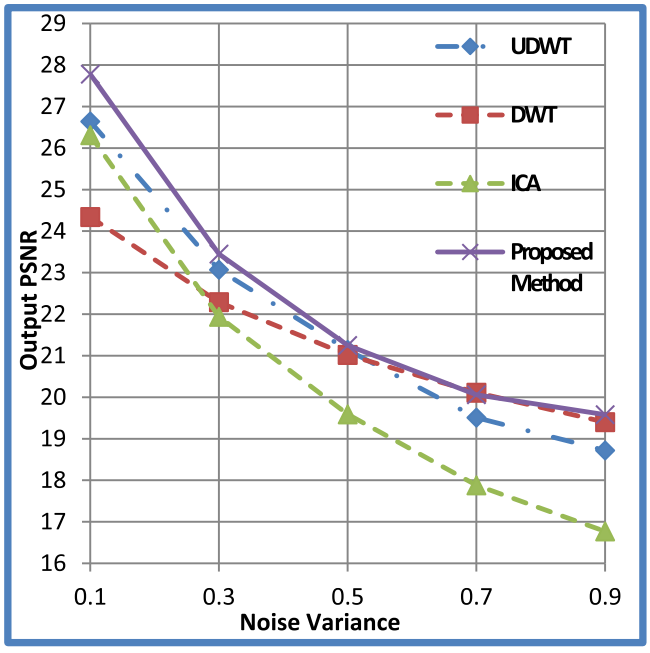

Fig. 5. Gaussian noise removal of MRI image in terms of PSNR.

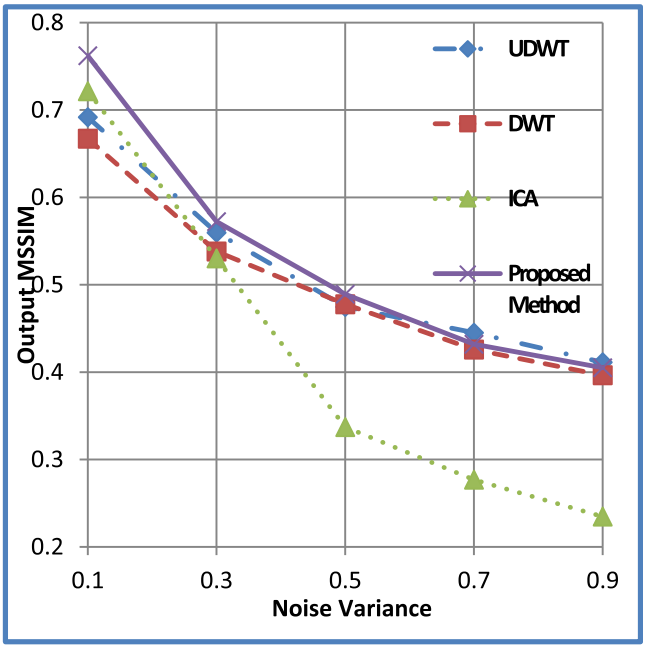

Fig. 6. Gaussian noise removal of MRI image in terms of MSSIM.

0.9 variance level, UDWT supersedes other transformation techniques even at proposed method in terms of MSSIM for Gaussian noise removal.

Table 1, visualizes the PSNR and MMSIM values for Gaussian noise removal. The PSNR and MSSIM values of noisy and denoised MRI images corrupted by Gaussian noise are tabulated for different noise levels (10–90%). The detailed comparison with state of art techniques, illustrate complete performances of Gaussian noise removal of MRI images using various denoising techniques with various noise variances. The tabulation result also shows that proposed method performs outstanding at lower noise levels, as compared to lower noise levels. For a noisy image with 0.1 noise variance have PSNR value of 20.96 dB, improves to 27.78 dB using proposed, which is found to be the best amongst PSNR obtained by other methods. The proposed method also improves the MSSIM of 0.4241of a noisy image at the same noise level to 0.7621 of the denoised image, which is highest among all.

The process was repeated for denoising of MRI images corrupted by speckle noise for different noise levels of 0.1–0.9), shown in Fig. 7. It visualizes that the proposed method provides the far better result as compared to other denoising techniques for every stage of noise level also the MSSIM result obtained by the proposed method is higher among all for speckle noise at every stage of noise density, shown in Fig. 8.

The PSNR values for speckle noise removal outperforms at each noise level whereas the MSSIM value using UDWT is approximately similar to proposed technique. That means the structural similarity maintained while speckle noise removal is nearly same for both UDWT and proposed method but noise removal metrics PSNR is far better that all other techniques used for comparison.

Table 2, tabulated the experimental result of denoising of speckle noise in more details. PSNR and MSSIM values of denoised images are much improved at the higher level at 0.9 noise variance from 20.22 to 25.58 dB and 0.6340 to 0.8026 as compared to the lower level at 0.1 noise variance from 29.63 to 30.15 dB and 0.8635 to 0.8795 by proposed method respectively.

The salt and pepper noise removal using DWT-ICA method gives far better result at higher noise variance. Mean structural similarity index metric value at higher noise level is very much improved,

Table 1
Denoising result for Gaussian Noise removal.

Noise Level	PSNR (Noisy)	PSNR (Denoised)	MSSIM (Noisy)	MSSIM (Denoised)
		UDWT		
0.1	20.96	26.64	0.4241	0.6917
0.3	16.43	23.07	0.2601	0.5597
0.5	14.39	21.14	0.1976	0.4747
0.7	13.19	19.51	0.1654	0.4451
0.9	12.34	18.72	0.1404	0.4113
		DWT		
0.1	20.96	24.34	0.4241	0.6672
0.3	16.43	22.29	0.2601	0.5381
0.5	14.39	21.02	0.1976	0.4777
0.7	13.19	20.11	0.1654	0.4259
0.9	12.34	18.40	0.1404	0.3964
		ICA		
0.1	20.96	26.31	0.4241	0.7215
0.3	16.43	21.94	0.2601	0.5303
0.5	14.39	19.59	0.1976	0.3372
0.7	13.19	17.88	0.1654	0.2769
0.9	12.34	16.77	0.1404	0.2347
		Proposed method		
0.1	20.96	**27.78**	0.4241	**0.7621**
0.3	16.43	**23.45**	0.2601	**0.5723**
0.5	14.39	**21.25**	0.1976	**0.4892**
0.7	13.19	**20.06**	0.1654	**0.4320**
0.9	12.34	**19.58**	0.1404	**0.4050**

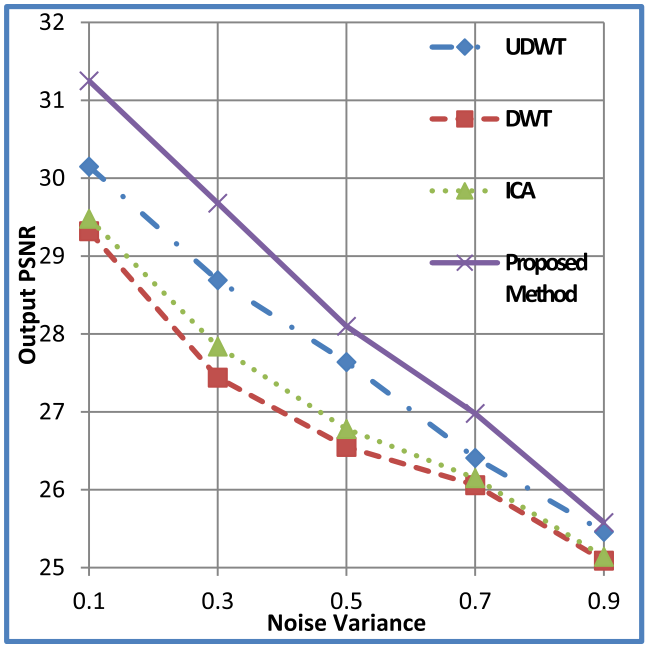

Fig. 7. Speckle noise removal of MRI image in terms of PSNR.

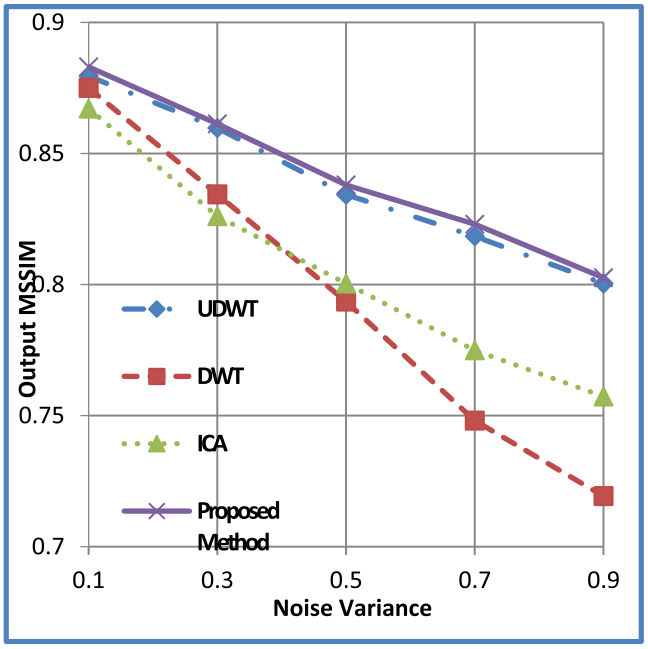

Fig. 8. Speckle noise removal of MRI image in terms of MSSIM.

that means it maintains the structural similarity better for salt and pepper noise removal.

Fig. 9 shows the result of salt & pepper noise removal in terms of PSNR values with various noise levels whereas as the graph between MSSIM and noise variance is plotted in Fig. 10. It is found that the proposed method gives the best result in term of both PSNR and MSSIM at each level of noise, however, DWT gives worst result among all for salt & pepper noise.

Table 3 tabulates the PSNR & MSSIM values obtained for noisy and denoised MRI images corrupted by salt & pepper noise. For each tested method, the results revealed that proposed technique produced the highest PSNR and MSSIM values as compared to other filtering techniques at various noise levels.

The denoised result of MR Images are tabulated in Tables 1–3 and it concludes that the proposed techniques gives better result in every aspect for removing all types of noise except for Gaussian noise removal. In the removal of Gaussian noise the UDWT maintains slightly better structure similarity as compared to all other transform domain techniques. The reason behind this is UDWT is having shift variant property which gives better accuracy as well smoothness as compared to DWT and ICA.

Over all result with proposed method (ICA-DWT) gives better result and also maintains the structure similarity at lower to higher noise level. So, the DWT offers worst result among all other techniques and UDWT gives 2nd best result among all denoising

Table 2
Denoising results for Speckle Noise removal.

Noise Level	PSNR (Noisy)	PSNR (Denoised)	MSSIM (Noisy)	MSSIM (Denoised)
		UDWT		
0.1	29.63	30.15	0.8635	0.8795
0.3	24.91	28.69	0.7595	0.8597
0.5	22.69	27.64	0.7055	0.8343
0.7	21.25	26.41	0.6643	0.8184
0.9	20.22	25.46	0.6340	0.8004
		DWT		
0.1	29.63	29.32	0.8635	0.8750
0.3	24.91	27.44	0.7595	0.8344
0.5	22.69	26.55	0.7055	0.7935
0.7	21.25	26.06	0.6643	0.7481
0.9	20.22	25.09	0.6340	0.7193
		ICA		
0.1	29.63	29.48	0.8635	0.8671
0.3	24.91	27.84	0.7595	0.8261
0.5	22.69	26.78	0.7055	0.8004
0.7	21.25	26.15	0.6643	0.7749
0.9	20.22	25.14	0.6340	0.7573
		Proposed method		
0.1	29.63	**31.25**	0.8635	**0.8830**
0.3	24.91	**29.68**	0.7595	**0.8613**
0.5	22.69	**28.10**	0.7055	**0.8380**
0.7	21.25	**26.98**	0.6643	**0.8230**
0.9	20.22	**25.58**	0.6340	**0.8026**

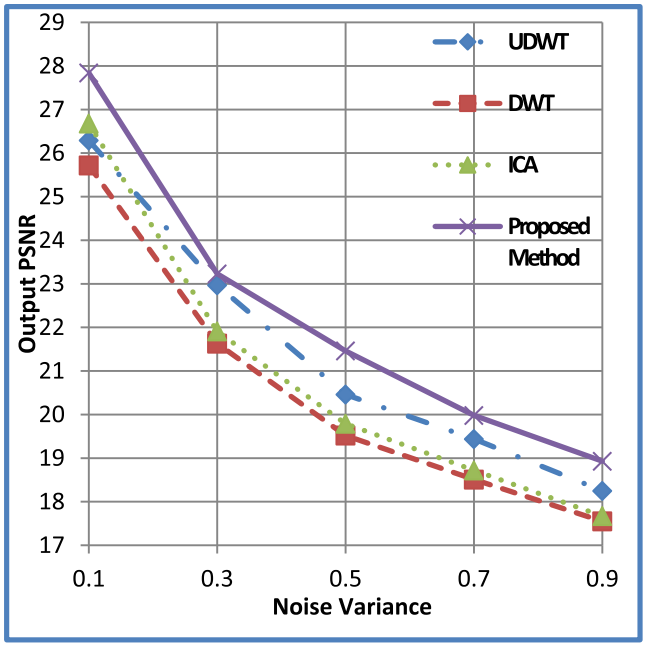

Fig. 9. Salt & pepper noise removal of MRI image in terms of PSNR.

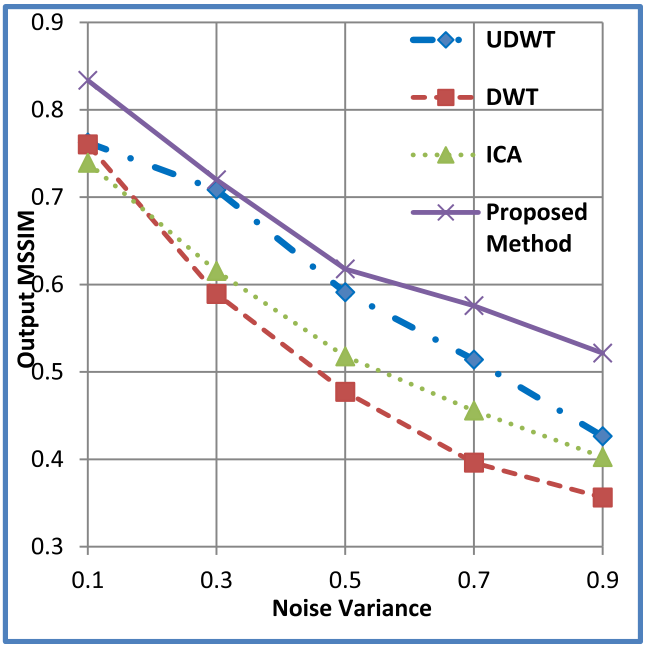

Fig. 10. Salt & pepper noise removal of MRI image in terms of MSSIM.

method used. But when DWT is combined with ICA as explained in section 5, it provides great result in terms of PSNR and MSSIM compare to UDWT, ICA and DWT. Because the decomposition capability of DWT further removed the noise after preprocessing steps applied using ICA.

Figs. 11–13 pictures the comparison result of the proposed method with other conventional methods such as UDWT, DWT, ICA with a noise variance of 0.1 corrupted by various noises. Fig. 11 shows the denoising result of MRI images corrupted by 10% of Gaussian noise using different filtering techniques. Figs. 12 and 13 picturizes the result of speckle noise and salt & pepper noise removal at 0.1 noise level of MRI images respectively. DWT-ICA method removes the noise effectively without losing the useful information of the image i.e. with high-value MSSIM. From the figures, it is also observed that the proposed method suppresses all the noises (Gaussian, speckle, salt & pepper) significantly with preserving the fine details. The result advocates that the proposed technique is robust for the removal of random noise while it also preserves the important information in the images.

7. Conclusion

A new hybrid adaptive technique using DWT-ICA for Noise reduction of Magnetic Resonance Images was proposed in this

Table 3
Denoising results for Salt & Pepper Noise removal.

Noise Level	PSNR (Noisy)	PSNR (Denoised)	MSSIM (Noisy)	MSSIM (Denoised)
		UDWT		
0.1	24.50	26.29	0.6260	0.7624
0.3	19.76	22.97	0.5949	0.7085
0.5	17.31	20.46	0.4514	0.5911
0.7	15.93	19.44	0.3572	0.5141
0.9	14.85	18.25	0.3073	0.4264
		DWT		
0.1	24.50	25.72	0.6260	0.7604
0.3	19.76	21.63	0.5949	0.5892
0.5	17.31	19.52	0.4514	0.4772
0.7	15.93	18.51	0.3572	0.3961
0.9	14.85	17.55	0.3073	0.3563
		ICA		
0.1	24.50	26.68	0.6260	0.7393
0.3	19.76	21.91	0.5949	0.6155
0.5	17.31	19.79	0.4514	0.5178
0.7	15.93	18.72	0.3572	0.4557
0.9	14.85	17.67	0.3073	0.4026
		Proposed method		
0.1	24.50	**27.84**	0.6260	**0.8337**
0.3	19.76	**23.23**	0.5949	**0.7200**
0.5	17.31	**21.46**	0.4514	**0.6178**
0.7	15.93	**19.98**	0.3572	**0.5758**
0.9	14.85	**18.93**	0.3073	**0.5215**

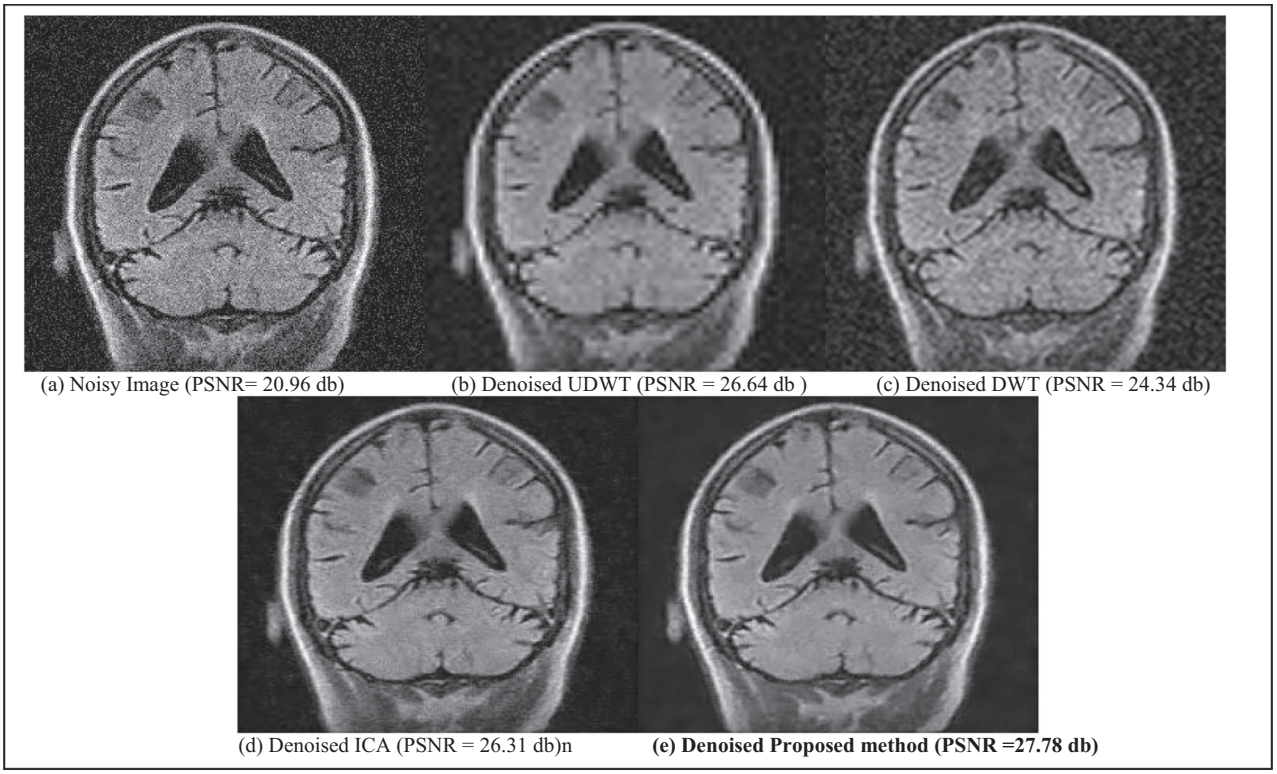

Fig. 11. Gaussian noise removal results at 0.1 variance level.

paper. The proposed technique uses a combination of independent component analysis and discrete wavelet transform for obtaining noise-free data. A database utilized for this work contains T1 weighted brain MRI images. The MRI image corrupted by Gaussian noise, speckle noise, salt & pepper noise with the noise variances of 0.1, 0.3, 0.5, 0.7 and 0.9 were denoised using the proposed method and obtained result is compared with state of art techniques such as UDWT, DWT, and ICA. Finally, the results obtained by the proposed algorithm were found best, among the other conventional transform methods used for denoising of MRI images. The output obtained from proposed method also has a higher PSNR and higher MSSIM value compare to the other methods used. The simulation results also reveal that DWT-ICA algorithm provides a far better result at a higher level of noise variance this method was also found better to preserve the structure of the MRI images, which is the most important concern when these images are used for

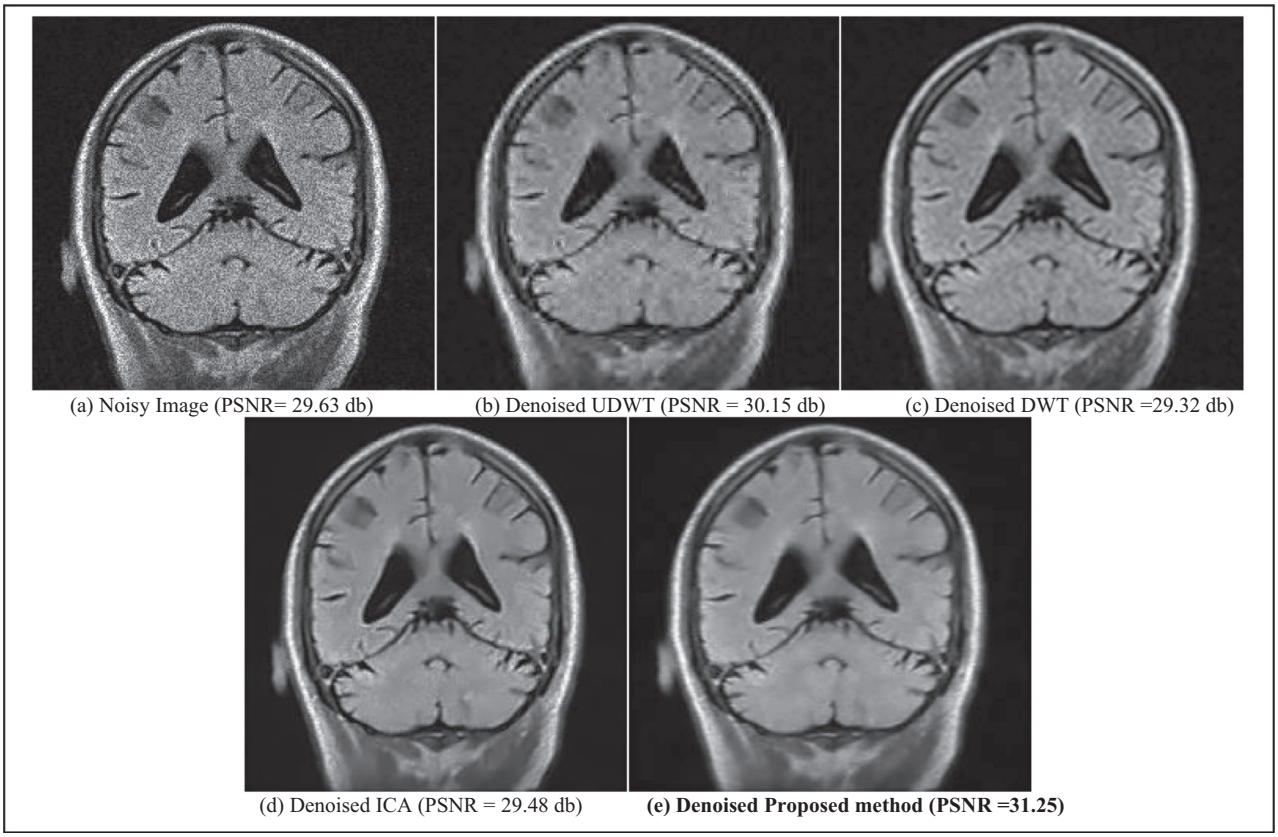

Fig. 12. Speckle noise removal results at 0.1 variance level.

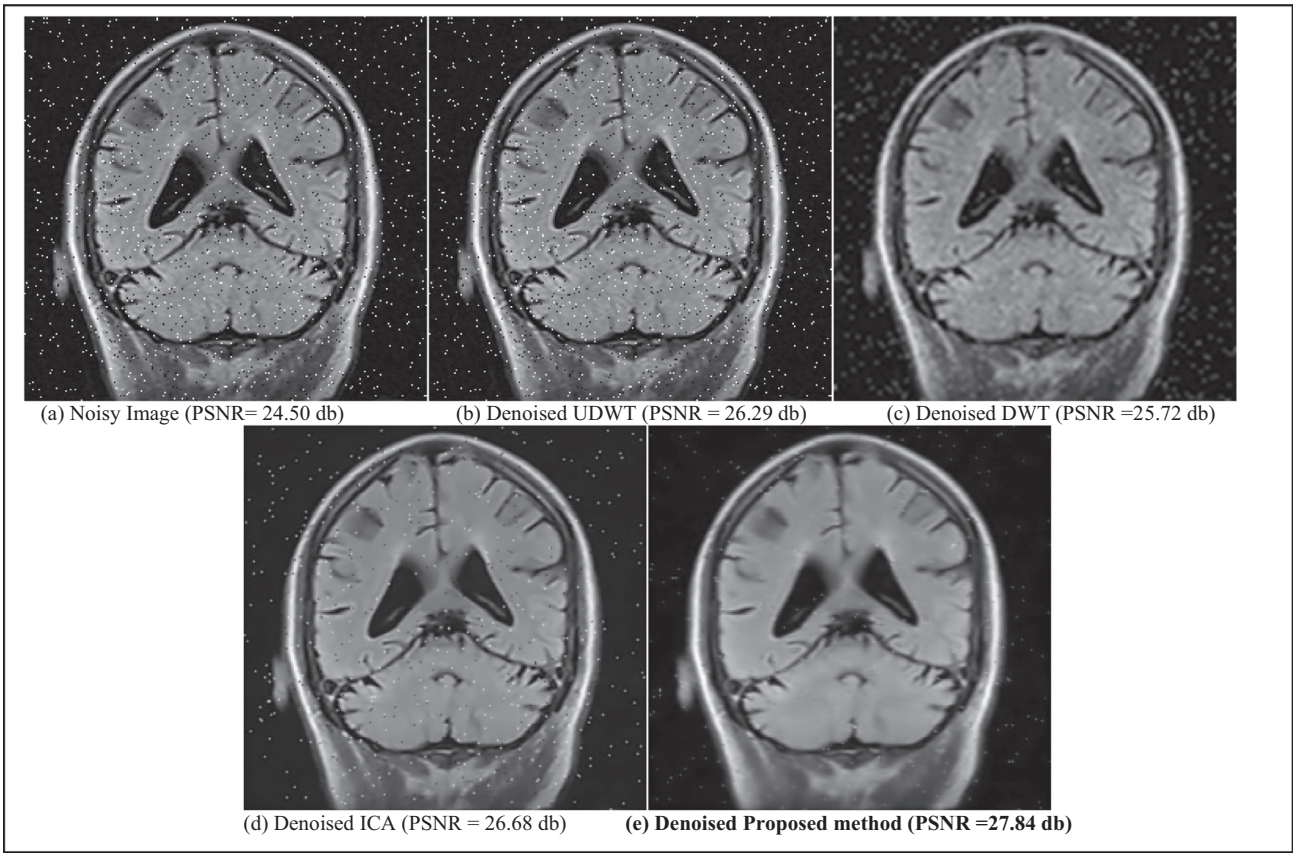

Fig. 13. Salt & Pepper noise removal results at 0.1 variance level.

diagnosis purpose. The proposed technique (DWT-ICA) was thus found to be a robust and efficient method for removal of random noise from MRI images.

Due to the limitlessness of the research area, this manuscript inept to describe the various methods and the comparison with SAR image analysis with medical image analysis, which is the recent area of research will be the future scope of this paper. Techniques such as sparse coding and spectral clustering based on UFL (unsupervised feature learning), kurtosis curvelet energy (KCE), fused radar and optical data classification, Cellular Learning Automata and Adaptive will be also surveyed in the future research [4,5,42,6,7,36–41].

Acknowledgments

We wish to express our sincere thanks to Capt. Sunil Sharma, Dr. S.M Chincholikar, Consultant Radiologist and Mr. Mangesh Ambhore "Charak Diagnostic and Research Centre", Jabalpur, M. P., India for providing us with different MR Image datasets. We also extend our deep gratitude to Dr. Shailja Shukla, Professor and Head Department of Computer Science and Engineering Jabalpur Engineering College, Jabalpur, M.P., India for helping us to collect the database and constant encouragement and concrete suggestions.

References

[1] A. Maity, A. Pattanaik, S. Sagnika, S. Pani, A Comparative Study on Approaches to Speckle Noise Reduction in Images, (2015). doi:10.1109/CINE.2015.36.
[2] A.K. Boyat, B.K. Joshi, A review paper: noise models in digital image processing, Sign. Image Proc.: An Int. J. (SIPIJ) 6 (2) (2015) 63–75.
[3] G. Akbarizadeh, A new statistical-based kurtosis wavelet energy feature for texture recognition of SAR images, IEEE Trans. Geosci. Remote Sens. 50 (2012) 4358–4368.
[4] D. karimi, G. Akbarizadeh, K. Rangzan, M. Kabolizadeh, Effective supervised multiple-feature learning for fused radar and optical data classification, IET Radar, Sonar & Navigat. 11 (5) (2017) 768–777, https://doi.org/10.1049/iet-rsn.2016.0346.
[5] Z. Tirandaz, G. Akbarizadeh, A two-phase algorithm based on kurtosis curvelet energy and unsupervised spectral regression for segmentation of SAR images, IEEE J. Select. Top. Appl. Earth Observ. Remote Sens. (2015) 1–21.
[6] M. Rahmani, G. Akbarizadeh, Unsupervised feature learning based on sparse coding and spectral clustering for segmentation of synthetic aperture radar images, IET Comput. Vis. 9 (5) (2015) 629–638, https://doi.org/10.1049/iet-cvi.2014.0295.
[7] D. Karimi, K. Rangzan, G. Akbarizadeh, M. Kabolizadeh, Combined algorithm for improvement of fused radar and optical data classification accuracy, J. Electron. Imaging 26 (1) (2017), https://doi.org/10.1117/1.JEI.26.1.013017, 013017.
[8] G. Salimi-khorshidi, G. Douaud, C.F. Beckmann, M.F. Glasser, L. Griffanti, S.M. Smith, NeuroImage automatic denoising of functional MRI data: combining independent component analysis and hierarchical fusion of classifiers, Neuroimage 90 (2014) 449–468, https://doi.org/10.1016/j.neuroimage.2013.11.046.
[9] J. Mohan, V. Krishnaveni, Y. Guo, A survey on the magnetic resonance image denoising methods, Biomed. Signal Process. Control. 9 (2014) 56–69, https://doi.org/10.1016/j.bspc.2013.10.007.
[10] D. Ai, J. Yang, J. Fan, W. Cong, X. Wang, Denoising filters evaluation for magnetic resonance images, Opt. - Int. J. Light Electron Opt. 126 (2015) 3844–3850, https://doi.org/10.1016/j.ijleo.2015.07.155.
[11] B. Liu, X. Sang, S. Xing, B. Wang, Noise suppression in brain magnetic resonance imaging based on non-local means filter and fuzzy cluster, Opt. - Int. J. Light Electron Opt. 126 (2015) 2955–2959, https://doi.org/10.1016/j.ijleo.2015.07.056.
[12] J. Hu, J. Zhou, X. Wu, Non-local MRI denoising using random sampling, Magn. Reson. Imaging 34 (2016) 990–999, https://doi.org/10.1016/j.mri.2016.04.008.
[13] X. Wang, S. Shen, G. Shi, Y. Xu, P. Zhang, Iterative non-local means filter for salt and pepper noise removal, J. Vis. Commun. Image Represent. 38 (2016) 440–450, https://doi.org/10.1016/j.jvcir.2016.03.024.
[14] M. Kumar, M. Diwakar, CT image denoising using locally adaptive shrinkage rule in tetrolet domain, J. King Saud Univ. – Comput. Inf. Sci. (2016), https://doi.org/10.1016/j.jksuci.2016.03.003.
[15] C.T. Lu, M.Y. Chen, J.H. Shen, L.L. Wang, C.C. Hsu, Removal of salt-and-pepper noise for X-ray bio-images using pixel-variation gain factors, Comput. Electr. Eng. (2017) 1–15, https://doi.org/10.1016/j.compeleceng.2017.08.012.
[16] F. Baselice, G. Ferraioli, V. Pascazio, A. Sorriso, Bayesian MRI denoising in complex domain, Magn. Reson. Imaging 38 (2017) 112–122, https://doi.org/10.1016/j.mri.2016.12.024.
[17] S. Gai, B. Zhang, C. Yang, L. Yu, Speckle noise reduction in medical ultrasound image using monogenic wavelet and Laplace mixture distribution, Digit. Signal Process. A Rev. J. 72 (2018) 192–207, https://doi.org/10.1016/j.dsp.2017.10.006.
[18] H. Zhu, J. Zhang, Z. Wang, Arterial spin labeling perfusion MRI signal denoising using robust principal component analysis, J. Neurosci. Methods 295 (2018) 10–19, https://doi.org/10.1016/J.JNEUMETH.2017.11.017.
[19] M. Diwakar, M. Kumar, Biomedical signal processing and control a review on CT image noise and its denoising, Biomed. Signal Process. Control. 42 (2018) 73–88, https://doi.org/10.1016/j.bspc.2018.01.010.
[20] P.V. Sudeep, P. Palanisamy, C. Kesavadas, J. Rajan, An improved nonlocal maximum likelihood estimation method for denoising magnetic resonance images with spatially varying noise levels, Pattern Recognit. Lett. (2018), https://doi.org/10.1016/J.PATREC.2018.02.007.
[21] MRI Database "Charak diagnostic & Research Center," Jabalapur, M.P., India. (n.d.). http://charakdnrc.com/mri.htmlb.
[22] D.W. McRobbie, E.A. Moore, M.J. Graves, M.R. Prince, MRI from picture to proton, 2006. doi:10.1017/CBO9780511545405.
[23] K. Möllenhoff, A.-M. Oros-Peusquens, N.J. Shah, Introduction to the basics of magnetic resonance imaging, in: G. Gründer (Ed.), Mol. Imaging Clin. Neurosci., Humana Press, Totowa, NJ, 2012, pp. 75–98, doi:10.1007/7657_2012_56.
[24] Luca Saba, Magnetic Resonance Imaging Handbook, CRC Press, (Taylor & Francis Group), Boca Raton, 2017.
[25] C. Constantinides, Magnetic Resonance Imaging: The Basics, CRC Press (Taylor & Francis), 2016.
[26] S.K. Behera, Fast Ica for Blind Source Separation and Its Implementation, 2009.
[27] C. Ruan, D. Zhao, W. Jia, C. Chen, Y. Chen, X. Liu, A new image denoising method by combining WT with ICA, Math. Probl. Eng. 2015 (2015) 1–9, https://doi.org/10.1155/2015/582640.
[28] K. Liang, J. Ye, ICA-based image denoising: a comparative analysis of four classical algorithms, in: 2017 IEEE 2nd Int. Conf. Big Data Anal. ICBDA 2017, 2017, pp. 709–713, doi:10.1109/ICBDA.2017.8078728.
[29] C. Singh, S.K. Ranade, K. Singh, Invariant moments and transform-based unbiased nonlocal means for denoising of MR images, Biomed. Signal Process. Control. 30 (2016) 13–24, https://doi.org/10.1016/j.bspc.2016.05.007.
[30] I.S. Isa, S.N. Sulaiman, M. Mustapha, S. Darus, Evaluating denoising performances of fundamental filters for T2-weighted MRI images, Procedia Comput. Sci. 60 (2015) 760–768, https://doi.org/10.1016/j.procs.2015.08.231.
[31] A. Hyvärinen, Fast and robust fixed-point algorithms for independent component analysis, IEEE Trans-Actions Neural Networks 10 (1999) 626–634, https://doi.org/10.1109/72.761722.
[32] M. Biswas, H. Om, A new soft-thresholding image denoising method, Procedia Technol. 6 (2012) 10–15, https://doi.org/10.1016/j.protcy.2012.10.002.
[33] F. Xiao, Y. Zhang, A comparative study on thresholding methods in wavelet-based image denoising, Procedia Eng. 15 (2011) 3998–4003, https://doi.org/10.1016/j.proeng.2011.08.749.
[34] National Instruments India, LabVIEW 2010 Advanced Signal Processing Toolkit Help, (n.d.). http://zone.ni.com/reference/en-XX/help/371419D-01/lvasptconcepts/wa_uwt/.
[35] H. ming Ni, D. wei Qi, H. Mu, Applying MSSIM combined chaos game representation to genome sequences analysis, Genomics 110 (2018) 180–190, https://doi.org/10.1016/j.ygeno.2017.09.010.
[36] M. Modava, G. Akbarizadeh, Coastline extraction from SAR images using spatial fuzzy clustering and the active contour method, Int. J. Remote Sens. 2 (2017) 355–370, https://doi.org/10.1080/01431161.2016.1266104.
[37] Q. Zhang, L.T. Yang, Z. Chen, Deep computation model for unsupervised feature learning on big data, IEEE Trans. Serv. Comput. 9 (2016) 161–171, https://doi.org/10.1109/TSC.2015.2497705.
[38] G. Akbarizadeh, Segmentation of SAR satellite images using cellular learning automata and adaptive chains, J. Remote Sensing Technol. 1 (2) (2013) 44–51, https://doi.org/10.18005/JRST0102003.
[39] M. Modava, A Level set based Method for Coastline Detection of SAR Images, (2017) 253–257.
[40] G. Akbarizadeh, A.E. Moghaddam, Detection of lung nodules in CT scans based on unsupervised feature learning and fuzzy inference, J. Med. Imaging Health Inform. 6 (2016) 477–483, https://doi.org/10.1166/jmihi.2016.1720.
[41] N. Ahmadi, G. Akbarizadeh, Hybrid robust iris recognition approach using iris image pre-processing, two-dimensional gabor features and multi-layer perceptron neural network/PSO, IET Biometrics 7 (2018) 153–162, https://doi.org/10.1049/iet-bmt.2017.0041.
[42] M. Farbod, G. Akbarizadeh, A. Kosarian, K. Rangzan, Optimized fuzzy cellular automata for synthetic aperture radar image edge detection, J. Electron. Imaging. 27 (2018), https://doi.org/10.1117/1.JEI.27.1.013030.